# APPLIED GEOSTATISTICS TO THE ASSESSMENT OF ENHANCED GEOTHERMAL SYSTEM (EGS) IN CENTRAL SUMATRA BASIN

## *APLIKASI GEOSTATISTIK UNTUK PENILAIAN POTENSI ENHANCED GEOTHERMAL SYSTEM (EGS) DI CEKUNGAN SUMATERA TENGAH*

**Josua Washington Sihotang[1] and Syaiful Alam[2]**
[1]Faculty of Geological Engineering Padjadjaran University,
[2]Laboratory of Stratigraphy Padjadjaran University
josua16005@mail.unpad.ac.id

## ABSTRACT

Thick sediment (over 2,500 m), fractured basement and high thermal gradient (up to 19.10 ºC/100 m) of Central Sumatra Basin are suitable factors to have the Enhanced Geothermal System (EGS) potential. A number of 130 wells data were used to evaluate EGS of the basin. The assessment is divided into the number of estimation within grid cell (1 km x 1 km) of sediment thickness, heat flow, thermal conductivity and technical potential calculated starting from basement-sediment layer interface. The distribution of heat flow and gradient thermal values correspond to the sediment layer. The autocorrelation test indicate the data is stationary. The variance of data gets bigger after a depth over 5.5 km. According to the Breadsmore protocol, the technical potential value ranged from 0.5 MW up to 4.7 MW at the depth of 3.5 km. In addition, the lowest technical potential is 0.66 MW and the highest is 5.76 MW at a depth of 4.5 km. The ordinary kriging, using number of lags 10 in variogram modeling, estimated the technical potential distribution is higher to the southwest.

**Keywords**: Enhanced Geothermal Systems (EGS), Central Sumatra Basin, Geostatistics

## *ABSTRAK*

*Ketebalan sedimen (lebih dari 2.500 m), rekahan pada batuan dasar, dan gradient thermal yang tinggi (mencapai 19,10 C/100 m) dari Cekungan Sumatera Tengah membuat cekungan ini memiliki potensi penggunaan Enhanced Geothermal System (EGS). Sebanyak 130 data sumur digunakan untuk mengevaluasi EGS dari cekungan. Penilaian dibagi ke dalam beberapa nomor estimasi di dalam grid cell (1 km x 1 km) dari ketebalan sedimen, heat flow, konduktivitas thermal, dan technical potential dihitung mulai dari muka lapisan batuan dasar dan batuan sedimen. Uji Autokorelasi mengindikasikan bahwa persebaran data bersifat stasioner. Varians data meningkat setelah kedalaman 5,5 km. Berdasarkan Beardsmore Protocol, nilai technical potential beragam mulai dari 0,5 MW – 4,7 MW pada kedalaman 3,5 km. Sebagai tambahan, nilai technical potential terendah sebesar 0,66 MW dan tertinggi 5,76 MW pada kedalaman 4,5 km. Ordinary Kriging, menggunakan besar lag-10 pada pemodelan variogram, mengestimasikan bahwa distribusi technical potential lebih tinggi terdapat di sebelah Barat Daya.*

***Kata kunci**: Enhanced Geothermal Systems (EGS), Cekungan Sumatra Tengah, Geostatistika*

## INTRODUCTION

As the world largest geothermal potential, Indonesia should be the most productive country in geothermal energy utilizing. It is estimated that Indonesia has 28,910 GW geothermal potential drawn from 312 fields in several islands (Pambudi, 2017). Unfortunately, Indonesia is only in the third rank for about 5% geothermal energy utilization ratio that shows a low utilization under USA and Philippine. Nowadays, the whole country in this world should develop the sustainable and clean energy to overcome the greenhouse gas (GHG) emission impact. The Indonesia government is committed to enhance the geothermal energy production for fossil fuel instead. Therefore, the methodology penetration is needed to enhance the geothermal production.

Enhanced Geothermal Systems (EGS) is a method that is used to artificially create the geothermal systems included hydrothermal resources that can be used to generate electricity. The conventional geothermal energy exploitation was limited to shallow and high-enthalpy reservoirs (>180 °C) in volcanic areas, whereas EGS technologies may exploit in medium-enthalpy reservoirs (80-180 °C) situated at greater depth in the basement rock (Limberger et al, 2014). Generally, geothermal energy is limited by the size and location of the reservoir and utilizes the natural reservoir. Consequently, EGS was needed to be utilized in which can reduce these constraints by artificially create the hydrothermal reservoirs in hot and deep geological formations, where energy production had not been economical.

Technically, EGS is worked by injecting the fluid into the subsurface under carefully controlled conditions, which is creating the artificial fractures to create the permeability (U. S. Department of Energy, 2012). EGS also may reduce the emission impact that is almost entirely free of greenhouse gas (GHG) emissions. Only when the drilling phase, EGS might be released the small traces of carbon dioxide and other GHGs. Economic EGS field usually related to oil-prolific basin because it requires deep and thick sedimentary basin and high heat flow characteristic.

The geothermal electrical generation capacity is approximately 3-4 GW and hence the installed base provides approximately 20,000 GW/h of electrical energy in the United States (U. S. Department of Energy, 2012). The heat source was created due to the subject of the East Pacific Rise under South-Western North America and was associated with uplift and extension of the Basin and Range. Thus, EGS's prospective area in the United States was concentrated in the higher heat flow area of the western region. EGS could provide the 100 GW of cost-competitive in the next 50 years in the United States (MIT, 2006). Based on those conditions, EGS is possible to be developed in Indonesia. Indonesia has a complex tectonic setting and tectonically stressed sedimentary basin as a fine target for EGS preliminary study (Hendrawan and Draniswari, 2016). Indonesian crust relatively had a good heat generation due to thick sediment and surrounded by the ring of fire. This research aims to analyse the assessment of EGS utilization in Central Sumatra Basin for Indonesia's future sustainable and clean energy.

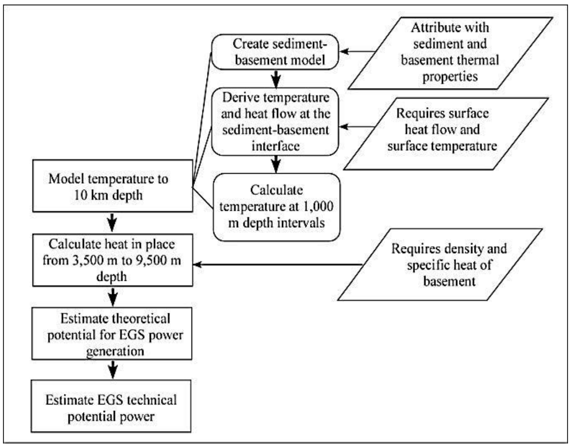


**Figure 1**. The Beardsmore Protocol workflow diagram (Busby and Terrington, 2017).

## METHODOLOGY

The surface and subsurface data were used to identify the suitability and calculate the EGS potential in Central Sumatra Basin. The assessment was done by using the Beardsmore Protocol (Beardsmore et al, 2010). The protocol recommends assessing the EGS potential from 3-10 km depth slice by creating the model of Basement-Sediment Interface and Basement rock (Busby and Terrington, 2017). The calculation then assisted by spatial statistics considering the data distribution and variogram modeling also kriging estimation to the depth target. The geostatistics approach mainly conducted to know the data distribution and spatial relationship. This research source was done by literature study from South East Asia Research Group (Table 1) to know the geological and heat characteristic of each well (Royal Holloway South East Asia Research Group, 2017).

The EGS potential calculating steps were compiled below based on the Beardsmore Protocol:

$Ts=To+[QoS/Ks]-As[S^2/2Ks]$.............(1)

Ts (°C) is the temperature at the sediment-basement interface To (°C) is the mean annual air temperature, Qo (W $m^{-2}$) is the surface heat flow, Ks (W $m^{-1}$ $K^{-1}$) is the sediment thermal conductivity, S (m) is the sediment thickness and As (W $m^{-3}$) is the sediment heat generation.

$Qs = Qo – S.As$.................................(2)

Qs (W $m^{-2}$) is the heat flow at the sediment–basement interface. The next step is to calculate the temperatures at depth of each 3000-9000 m depth slice.

$Tx=Ts+[(Qs(X-S))/Kb]-Ab[(X-S)^2/2Kb]$(3)

Tx (°C) is the temperature at depth X, Kb (W $m^{-1}$ $K^{-1}$) is basement thermal conductivity, and Ab (W $m^{-3}$) is the basement heat generation. According to the protocol, EGS potential is best to calculate within the basement rock.

$H= \rho\ Cp\ Vc\ (Tx-Tr)\times 10^{-18}$....................(4)

Where, H (Exajoule) is the Total Heat in Place, ρ (kg $m^{-3}$) is the density, Cp (J $kg^{-1}$ $K^{-1}$) is the specific heat of the basement cell, Vc ($m^3$) is the volume of the cell, Tx (°C) is the temperature at depth X and Tr = To + 80 (°C) is the mean annual air temperature. Theoretical potential assumed that the lifespan of power generation is 30 years (9.46 × 108 s). In which the Tx value is less than Tr, The H value may be negative and could be set to zero.

$P=(\eta th\ H \times 10^{12})/(9.46 \times 10^8\ )$............(5)

P is the Theoretical Potential EGS power in (MW), and ηth, is a function of inlet temperature.

$\eta th=0.00052Tx+0.032$.......................(6)

The technical potential power can be calculated after determining the technical limitations (Rybach, 2010). It was assumed that this efficiency value is 1.

$PT=1.057 \times P \times R$.................................(7)

Technical Potential (PT) for each basement cell (MW, megawatts). The R-value for the Beardsmore technical potential is 0.01 (Van Wees et al, 2013).

## GEOLOGY

The research area is located in a part of Central Sumatra Basin (Figure 2). This basin is called as back-arc basin that is formed by convergent activity between the Eurasian continental plate and Indo-Australian oceanic plate. The basin was formed as a NW-SE separated basin called dextral strike-slip faulting and had experienced in three tectonic deformation phases that are Eocene-Oligocene, Mesozoic compressional extensional, and Pliocene-Pleistocene compressional tectonics. Furthermore, Central Sumatra Basin has a high gradient geothermal because of the crustal fractures penetrating to the upper mantle (Eubank and Makki, 1981).

Heidrick and Aulia (1993) unveil the dominated strucutral fault in Central Sumatera Basin by two prominent fault sets. The more prevalent set strikes NW-SE and the other N-S. It is generally accepted that the N-S set is older and Paleogene in age. Eubank and Makki (1981) emphasized that both sets were repeatedly active during the Tertiary, and required to account for the disposition of Pematang grabens and half-grabens, also represent fundamental basement breaks in response to back-arc tension and dextral wrenching throughout the Tertiary. Structural styles and resulting deformational geometries that are diagnostic, statistically unique, form temporally distinct families including Beruk, Sumateran, Zamrud-Pedada and Bengkalis (Heidrick and Aulia, 1993).


**Figure 2**. The research area in a part of Central Sumatra Basin

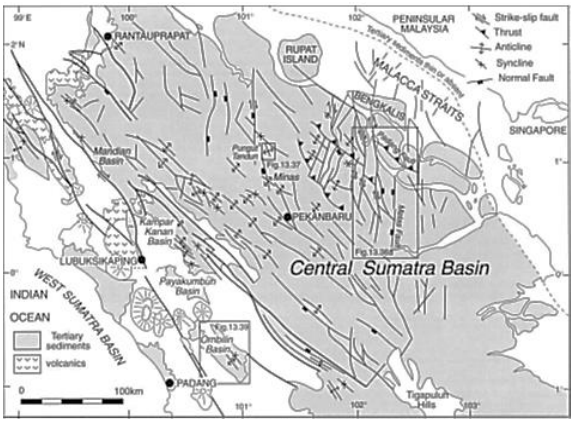


**Figure 3**. Geological structure in Central Sumatra Basin (Heidrick and Aulia, 1993)

Sedimentary process in Central Sumatra Basin was started at the beginning of Tertiary (Paleogene). Basement rock in Central Sumatra Basin is composed of (Eubank and Makki, 1981):

- Mallaca Terrane (Quartz Group) that is composed of quartzite, argillite, limestone crystalline and plutonic granite and granodiorite in Jura's age.
- Mutus assemblages that are composed of radiolarian chert, meta-argillite, red shale, limestone, and basaltic rocks.
- Mergui Terrane that is composed of greywacke, pebbly-mudstone, and quartzite from the Bahorok Formation. It is also found argillite, phyllite, limestone, and tuff from Kluet Formation.
- Kualu Terrane that is composed of phyllite, slate, tuff, and limestone.

There are 130 wells that were drilled, (Table 1), in this basin which are shown in modeled of technical potential (Figure 6) and (Figure 7). Gradient temperature, heat flow, sediment thickness, and thermal conductivity data were identified through the drillings and being modeled (Figure 4). The highest heat flow value can be found in the southwest area and decrease to the northeast. The highest surface heat flow (Qo) value is 0.356 Wm$^{-2}$ and the lowest is 0.083 W m$^{-2}$. It is directly proportional to the EGS potential. The largest sediment thickness (S) value is 2,542 m and the lowest is 287 m. The sediment thermal conductivity (Ks) data were ranged from 1.83–2.6 W m$^{-1}$. The gradient geothermal values were ranged from 37–191oC km-1.

## RESULT AND DISCUSSION

### RESULT

The temperature at 3.5 km and 4.5 km depths were determined before the technical potential calculation. The temperature at 3.5 km and 4.5 km depths were ranged in 104-326 $^{o}$C and 121-402 $^{o}$C, respectively. Some of these temperatures were classified as high geothermal systems (>150 $^{o}$C). The highest temperature can be found in the southwest region.

**Table 1**. The drillings data from 130 wells around the research area (Royal Holloway South East Asia Research Group, 2017)

| Latitude | Longitude | Well Name | Heat Flow (mW/m2) | Sediment Thickness (m) | Thermal Conductivity (W/m) | Gradient Temperature (oC/km) |
|---|---|---|---|---|---|---|
| 4.01 | 99.248333 | ASAHAN F | 83 | 995 | 2.23 | 185.09 |
| 3.595 | 99.28 | NSO-2S | 114 | 581 | 1.97 | 224.58 |
| 1.561667 | 100.943333 | UJUNG PA | 227 | 552 | 2.54 | 576.58 |
| 1.328333 | 100.001667 | TANAH UD | 117 | 1267 | 1.89 | 221.13 |
| 2.446667 | 100.231667 | PANAI-1 | 127 | 1567 | 2.15 | 273.05 |
| 1.888333 | 100.285 | PINGANGA | 98 | 963 | 2.09 | 204.82 |
| 1.235 | 100.253333 | GERINGGI | 106 | 1372 | 1.88 | 199.28 |
| 1.173333 | 100.106667 | KUMU-1 | 174 | 741 | 1.91 | 332.34 |
| 2.248333 | 100.336667 | BARUMUN- | 118 | 1690 | 2.48 | 292.64 |
| 2.136667 | 100.468333 | TOLANG-1 | 112 | 1578 | 2.06 | 230.72 |
| 2.103333 | 100.36 | DAUN-1 | 114 | 1262 | 2.09 | 238.26 |
| 2.061667 | 100.386667 | KARANG-1 | 141 | 1231 | 2.01 | 283.41 |
| 1.996667 | 100.481667 | SITANGKO | 154 | 579 | 1.97 | 303.38 |
| 1.996667 | 100.481667 | SITANGKO | 126 | 973 | 2.09 | 263.34 |
| 2.036667 | 100.533333 | TANJUNGK | 103 | 1853 | 2.15 | 221.45 |
| 1.876667 | 100.433333 | KUBU-3 | 118 | 422 | 2.36 | 278.48 |
| 1.786667 | 100.426667 | KUBU-2 | 114 | 1349 | 2.27 | 258.78 |
| 1.726667 | 100.441667 | TANJUNG | 105 | 1065 | 2.21 | 232.05 |
| 2.543333 | 100.523333 | TANJUNG | 104 | 845 | 2.2 | 228.8 |
| 2.655 | 100.465 | BUAYA-1 | 147 | 941 | 2.19 | 321.93 |
| 1.511667 | 100.346667 | KEBARO-1 | 124 | 1247 | 2.09 | 259.16 |
| 1.401667 | 100.406667 | MAHATO-1 | 118 | 1324 | 1.9 | 224.2 |
| 1.061667 | 100.383333 | TOBAT-1 | 172 | 593 | 1.89 | 325.08 |
| 2.893333 | 100.355 | PINANG-1 | 148 | 1251 | 2.04 | 301.92 |
| 1.956667 | 100.75 | DAMAR-1 | 119 | 1739 | 2.1 | 249.9 |
| 1.886667 | 100.755 | PINANG S | 129 | 1501 | 2.07 | 267.03 |
| 1.753333 | 100.7 | BALAM F | 127 | 1302 | 1.99 | 252.73 |
| 1.558333 | 100.626667 | TANJUNG | 158 | 718 | 2.13 | 336.54 |
| 1.251667 | 100.6 | TANGAH-1 | 111 | 1614 | 1.89 | 209.79 |
| 1.015 | 100.625 | KIRI-1 | 100 | 1730 | 1.88 | 188 |
| 0.786667 | 100.643333 | KOTALAMA | 198 | 990 | 2.11 | 417.78 |
| 0.66 | 100.623333 | LANGGAK- | 113 | 450 | 1.98 | 223.74 |
| 0.646667 | 100.706667 | KASIKAN- | 131 | 360 | 1.97 | 258.07 |
| 0.615 | 100.751667 | TERANTAM | 162 | 309 | 2.15 | 348.3 |
| 2.053333 | 100.778333 | ROKAN-1 | 118 | 1868 | 2.23 | 263.14 |
| 1.92 | 100.915 | BANTAIAN | 113 | 465 | 2.33 | 263.29 |
| 1.756667 | 100.82 | BANGKO F | 143 | 1047 | 2.03 | 290.29 |
| 1.641667 | 100.908333 | SERUNI F | 156 | 946 | 1.98 | 308.88 |
| 0.58 | 100.955 | SINTONG | 141 | 1112 | 2 | 282 |
| 1.505 | 100.885 | TELINGA- | 99 | 1443 | 1.98 | 196.02 |
| 1.473333 | 100.935 | SIKLADI | 99 | 1661 | 2.01 | 198.99 |
| 1.38 | 100.98 | KOPAR-1 | 119 | 1726 | 1.98 | 235.62 |
| 1.323333 | 100.803333 | JORANG F | 120 | 2223 | 2.01 | 241.2 |
| 0.905 | 101.055 | LIBO SE- | 115 | 1872 | 1.91 | 219.65 |
| 1.28 | 101.926667 | RANGAU F | 115 | 2542 | 2.01 | 231.15 |
| 1.123333 | 100.916667 | SIALANG- | 123 | 1994 | 1.94 | 238.62 |
| 1.043333 | 100.878333 | WADUK-1 | 114 | 2020 | 1.94 | 221.16 |
| 1.021667 | 100.838333 | HITAM-1 | 102 | 2029 | 1.93 | 196.86 |
| 0.986667 | 100.931667 | TAMALUKU | 106 | 1913 | 1.94 | 205.64 |
| 0.87 | 100.796667 | MAWAR-1 | 98 | 2041 | 1.94 | 190.12 |
| 0.78 | 100.918333 | LANCANG- | 114 | 2155 | 1.94 | 221.16 |
| 0.738333 | 100.78 | LINDAI-3 | 220 | 352 | 2.01 | 442.2 |
| 0.646667 | 100.876667 | SURAM-2 | 186 | 600 | 2.01 | 373.86 |
| 0.616667 | 101.001667 | PETAPAHA | 100 | 1544 | 1.94 | 194 |
| 0.598333 | 100.83 | KUSAN-1 | 120 | 663 | 1.94 | 232.8 |
| 0.491667 | 100.871667 | BIRUANG- | 153 | 499 | 2 | 306 |
| 2.273333 | 101.003333 | SENEBUI- | 108 | 586 | 2.07 | 223.56 |
| 2.231667 | 101.146667 | CSB-A1 | 90 | 758 | 2.04 | 183.6 |
| 1.931667 | 101.141667 | SEMENANJ | 97 | 643 | 2.17 | 210.49 |

| | | | | | | |
|---|---|---|---|---|---|---|
| 1,736667 | 101,005 | UJUNG TA | 173 | 779 | 1,98 | 342,54 |
| 1,565 | 101,115 | RANTAUBA | 134 | 988 | 2,15 | 288,1 |
| 1,61 | 101,128333 | KERBAU-1 | 122 | 1220 | 2,02 | 246,44 |
| 1,481667 | 101,095 | TINGGI-1 | 140 | 731 | 2,08 | 291,2 |
| 1,32 | 101,215 | DURI NE- | 139 | 609 | 2,12 | 294,68 |
| 1,37 | 101,135 | PETANI N | 103 | 1090 | 2,02 | 208,06 |
| 1,34 | 101,055 | PETANI-1 | 102 | 1457 | 2,05 | 209,1 |
| 1,283333 | 101,08 | PEMATANG | 130 | 1981 | 2,1 | 273 |
| 1,203333 | 101,123333 | PEMATANG | 111 | 2347 | 2,03 | 225,33 |
| 1,191667 | 101,081667 | PUDU FIE | 118 | 2098 | 1,99 | 234,82 |
| 1,096667 | 101,216667 | PINGGIR | 127 | 1305 | 2,02 | 256,54 |
| 0,07 | 101,105 | SANGSAM- | 128 | 2106 | 1,9 | 243,2 |
| 0,68 | 101,195 | KOTAGARO | 115 | 1872 | 1,89 | 217,35 |
| 0,686667 | 101,105 | KOTABATA | 116 | 1581 | 1,92 | 222,72 |
| 0,535 | 101,04 | BATU-1 | 102 | 1334 | 1,92 | 195,84 |
| 0,428333 | 101,178333 | KAMPAR-1 | 112 | 1430 | 1,92 | 215,04 |
| 0,336667 | 101,018333 | BANGKINA | 210 | 561 | 2,33 | 489,3 |
| 0,223333 | 101,19 | LIPAI-1 | 142 | 964 | 2,17 | 308,14 |
| 1,92 | 101,275 | BULUHALA | 161 | 405 | 1,94 | 312,34 |
| 1,851667 | 101,303333 | PASIR-1 | 134 | 495 | 2,04 | 273,36 |
| 1,756667 | 101,441667 | DUMAI-2 | 145 | 607 | 2,01 | 291,45 |
| 1,663333 | 101,441667 | DUAMI-1 | 166 | 451 | 2,04 | 338,64 |
| 1,601667 | 101,243333 | MUTUS-1 | 142 | 1014 | 1,96 | 278,32 |
| 1,39 | 101,265 | LEBAN-1 | 185 | 610 | 1,99 | 368,15 |
| 1,155 | 101,3 | SEMUNAI | 187 | 604 | 2,06 | 385,22 |
| 1,053333 | 101,291667 | TANDUN F | 117 | 1180 | 1,99 | 232,83 |
| 0,895 | 101,236667 | MINDAL F | 131 | 1166 | 1,94 | 254,14 |
| 0,761667 | 101,438333 | MINAS FI | 157 | 945 | 1,92 | 301,44 |
| 1,88 | 101,465 | SAHIR-1 | 127 | 563 | 2,06 | 261,62 |
| 1,765 | 101,55 | RUPAT-1 | 149 | 287 | 1,94 | 289,06 |
| 1,73 | 101,678333 | MESIM-1 | 109 | 1095 | 1,93 | 210,37 |
| 1,655 | 101,633333 | PELETUNG | 147 | 449 | 1,97 | 289,59 |
| 1,336667 | 101,556667 | BAGANBEL | 162 | 550 | 2,09 | 338,58 |
| 0,995 | 101,64 | MERAK-1 | 124 | 1513 | 2,09 | 259,16 |
| 0,9 | 101,633333 | GARIB-1 | 109 | 1532 | 1,95 | 212,55 |
| 0,705 | 101,58 | PERAWANG | 135 | 990 | 1,9 | 256,5 |
| 0,54 | 101,54 | MINAS SO | 135 | 1162 | 1,98 | 267,3 |
| 0,521667 | 101,576667 | BARU-2A | 147 | 975 | 1,92 | 282,24 |
| 1,318333 | 101,776667 | SEMBILAN | 194 | 393 | 2,6 | 504,4 |
| 0,728333 | 101,881667 | KEUTAPAN | 149 | 799 | 1,88 | 280,12 |
| 0,671667 | 101,778333 | GASIP-1 | 153 | 1293 | 2,04 | 312,12 |
| 0,406667 | 101,836667 | LAGO-1 | 122 | 1197 | 1,87 | 228,14 |
| 0,176667 | 101,813333 | PENAR-1 | 105 | 1297 | 1,86 | 195,3 |
| 1,353333 | 102,148333 | PAKNING | 189 | 864 | 2,01 | 379,89 |
| 1,238333 | 102,101667 | SIAK KEC | 172 | 509 | 1,9 | 326,8 |
| 1,145 | 102,078333 | PEDADA-1 | 238 | 426 | 2,09 | 497,42 |
| 1,043333 | 102,055 | TASIB-1 | 197 | 791 | 2,3 | 453,1 |
| 0,981667 | 102,021667 | RAYA-1 | 143 | 849 | 2,08 | 297,44 |
| 0,81 | 102,028333 | DASAN-1 | 136 | 1469 | 2,04 | 277,44 |
| 0,771667 | 102,011667 | RAMBAH-1 | 186 | 766 | 1,96 | 364,56 |
| 0,685 | 101,965 | BUATAN-1 | 146 | 882 | 1,92 | 280,32 |
| 0,626667 | 102,06 | BERUK FI | 260 | 592 | 1,89 | 491,4 |
| 0,491667 | 102,05 | OTAK-1 | 164 | 871 | 1,91 | 313,24 |
| 0,185 | 102,093333 | TATAK-1 | 103 | 1673 | 1,88 | 193,64 |
| 1,161667 | 102,195 | GUNTUNG- | 141 | 1173 | 1,99 | 280,59 |
| 0,935 | 102,125 | PUSAKA-1 | 117 | 1715 | 2 | 234 |
| 0,598333 | 102,26 | ZAMRUD-1 | 158 | 1017 | 1,93 | 304,94 |
| 0,655 | 102,14 | BUNGSU F | 153 | 679 | 1,93 | 295,29 |
| 0,33 | 102,286667 | SALAK-1 | 113 | 1798 | 1,98 | 223,74 |
| 2,416667 | 99,75 | 1 | 111 | 572 | 2,1 | 233,1 |
| 2,816667 | 100,05 | 4 | 85 | 2175 | 2,13 | 181,05 |
| 1,05 | 100,3 | 8 | 365 | 274 | 1,9 | 693,5 |
| 2 | 100,466667 | 19 | 138 | 744 | 2,12 | 292,56 |
| 1,966667 | 100,666667 | 26 | 135 | 1250 | 2,02 | 272,7 |
| 1,866667 | 100,65 | 27 | 108 | 1204 | 1,72 | 185,76 |
| 0,716667 | 100,616667 | 30 | 124 | 488 | 1,97 | 244,28 |
| 0,633333 | 100,616667 | 32 | 150 | 496 | 1,83 | 274,5 |
| 1,933333 | 100,916667 | 37 | 139 | 914 | 2,06 | 286,34 |
| 1,7 | 100,75 | 38 | 140 | 799 | 2,08 | 291,2 |
| 1,65 | 100,8 | 39 | 124 | 2291 | 2,08 | 257,92 |
| 1,7 | 100,9 | 41 | 135 | 1198 | 3,12 | 421,2 |

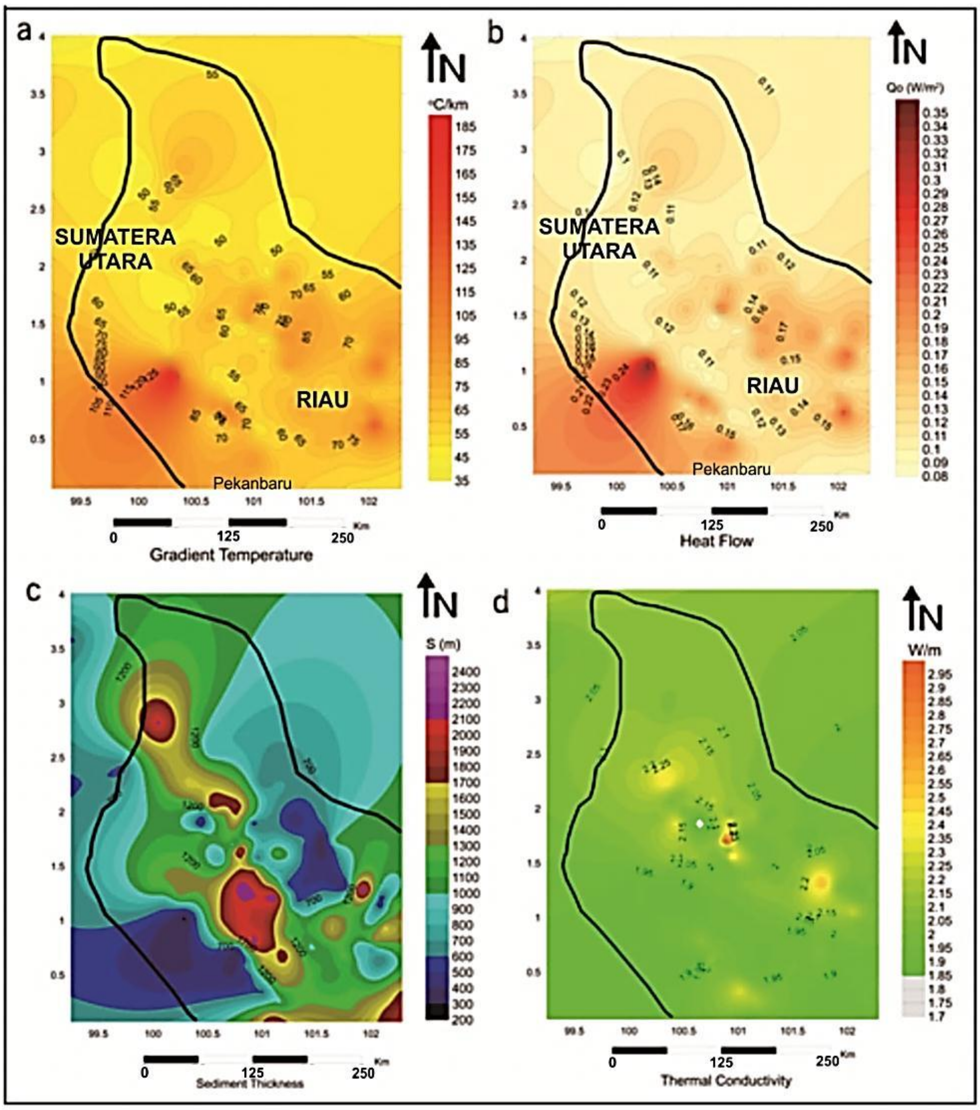


**Figure 4**. Modeled of a) gradient temperature b) heat flow c) sediment thickness d) thermal conductivity

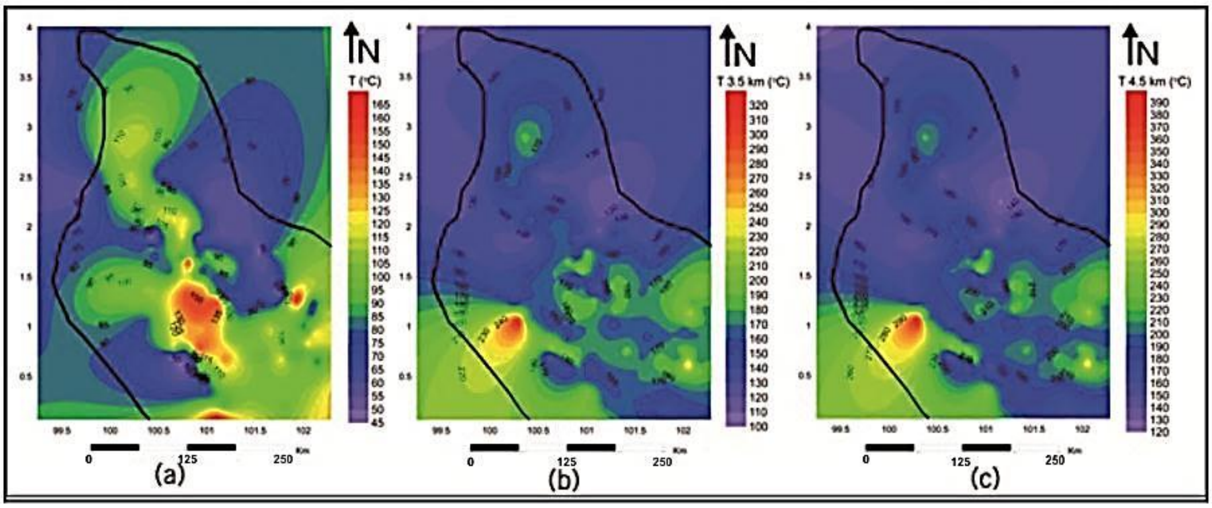


**Figure 5**. Modeled temperature at depth of a) basement-sediment interface b) 3.5 km c) 4.5 km

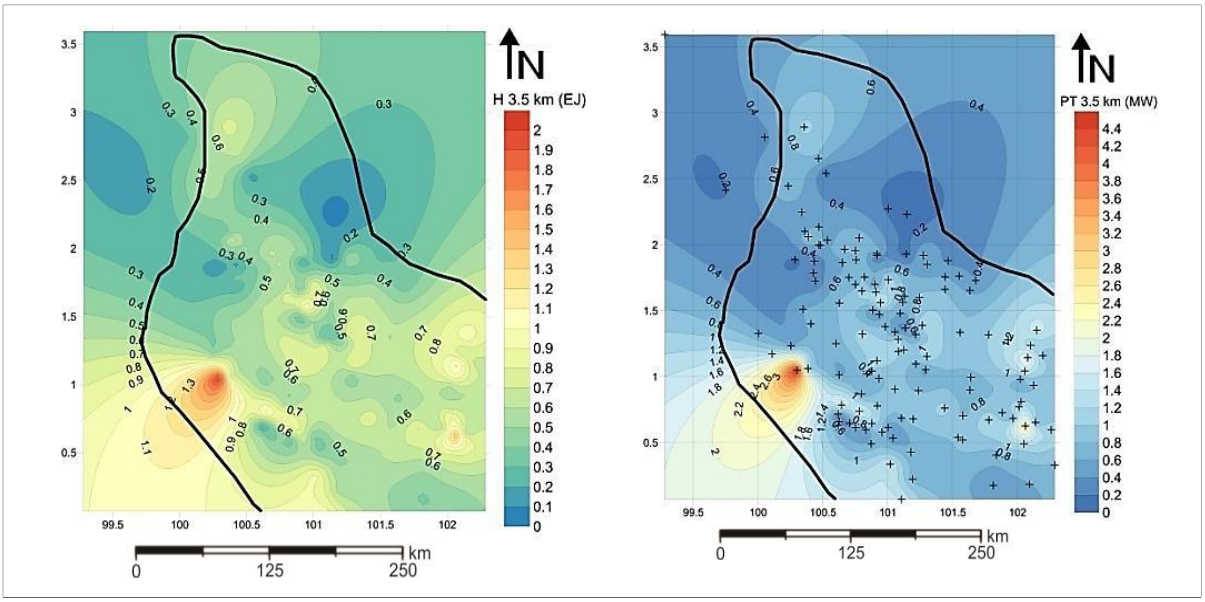


**Figure 6**. Modeled of a) heat in place at 3.5 km depth
b) technical potential at 3.5 km depth

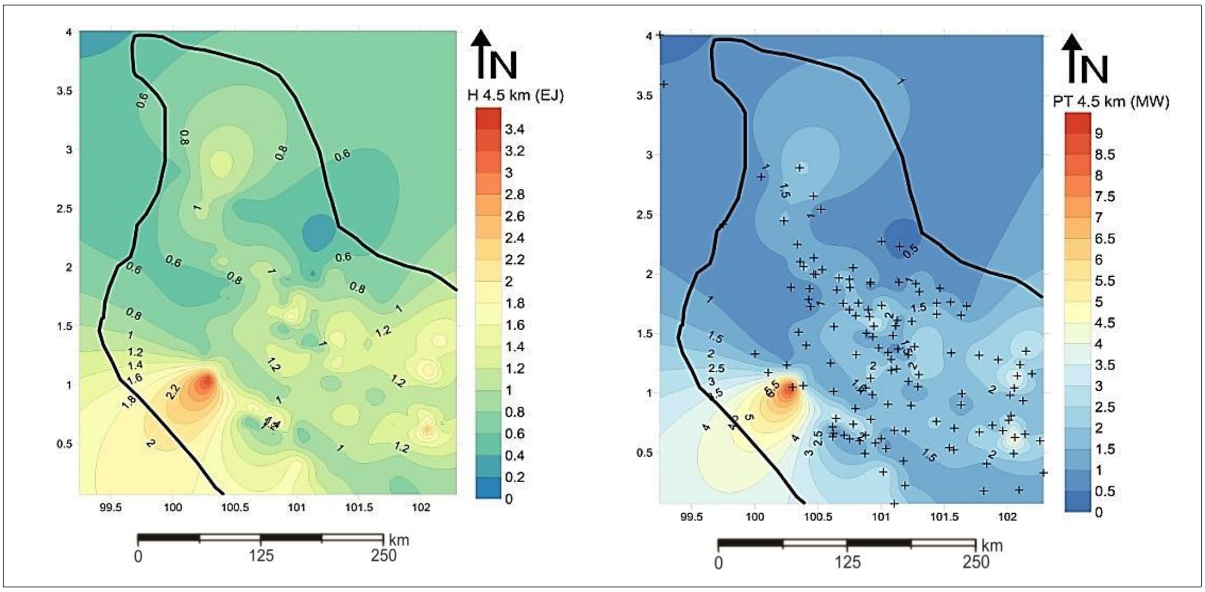


**Figure 7**. Modeled of a) heat in place at 4.5 km depth
b) technical potential at 4.5 km depth

The potential calculations were determined for each cell with 1 km x 1 km size. It was assumed that sediment heat generation (As) value was 1 W $m^{-3}$ and the specific heat of the basement cell (Cp) value was 1000 J/kg$^{o}$C (MIT, 2006). The basement rock was metamorphic rock that is rich in quartz. This lithology has the Kb value is 4.71 W $m^{-1}$ $K^{-1}$ (Clauser, 2006) due to the lithology was rich in quartz and Ab value is 1.35 W $m^{-3}$ (Slagstad, 2008).

The technical potential was assessed in 3.5 km and 4.5 km depths due to the thickest sediment was 2,542 m and the basement rock could produce higher heat generation than sedimentary rock. The calculation of technical potential was used the thermal efficiencies for a range of inlet fluid temperatures from 150 °C to 350 °C (MIT, 2006).

**TECHNICAL POTENTIAL AT 3.5 KM DEPTH**

The lithology at this depth was estimated as basement rock, which is the target for the drilling. This depth is related to the heat generation of basement rock with the various patterns. The total of Heat in Place of each well is 66.05 EJ. The Theoretical Potential is ranging from 47.4 - 444.68 MW. The lowest Technical Potential in this depth is 0.5 MW and the highest is 4.7 MW. The total of technical potential of each well is 103.5 MW.

**TECHNICAL POTENTIAL AT 4.5 KM DEPTH**

This depth slice was recommended to drill due to the economical properties. The total Heat in Place of each well is 131.66 EJ. The Theoretical Potential is ranging from 64.78–545.45 MW. The lowest Technical Potential is 0.66 MW and the highest is 5.76 MW. The total of Technical Potential is 217.9 MW that is available to fulfill the energy demands of Central Sumatra Area.

**GEOSTATISTICAL ANALYSIS**

**Data Distribution**

The technical potential distribution were evaluated from 3.5 km to 9.5 km depth. The data distribution was showed by histogram. The bar charts plotting were made on 4 types of depth slice in order to know the variance value through the deeper depth (Figure 8). The variance value visualize the Technical Potential data distribution of each well. From the geostatistical histogram analysis, the variance data was relatively show the significant different between 4.5 km, 5.5 km, and 6.5 km depth. The variance deviation data in each of the depth is 2.361 (for 4.5 km to 5.5 km depth) and 5.4929 (for 5.5 km to 6.5 km depth). These value was significantly different with variance data in 3.5 km to 4.5 km depth that is 0.8492. Thus, the recommendation depth to be drilled is in 3.5 and 4.5 km depth due to the small variance in deviation data. Moreover, the mean data from all of the 130 wells in 3.5 and 4.5 km depth is 0.8 MW and 1.6708 MW with the median is 0.7258 MW and 1.5199 MW, respectively. After data distribution reflecting the technical depth variables (3.5 km and 4.5 km) are analyzed, the spatial relationship between those variables should be considered. The way to check are consist of covariance, coefficient correlation and variogram. To generate them, the data condition (stationary or non-stationary) are authorized by autocorrelation test. Autocorrelation is a statistical test under the assumption either stationary or non-stationary data. It is also known as serial correlation of random process with a delayed lag of itself. The following equation is simply explaining the autocorrelation function;

$$R(\tau)=(E[(X_t-\mu)(X_{t+\tau}-\mu)])/\sigma^2 \text{.....................(8)}$$

with;

| | |
|---|---|
| $R(\tau)$ | = autocorrelation amplitude |
| $\tau$+t | = time-lag |
| E | = expected value operator |
| T | = discrete time |
| M | = mean |
| $\sigma^2$ | = variance |

About 60 time-lag were choosen to test stationary condition or randomness of the data as shwon in figure attachment. The amplitude of autocorrelation decrease rapidly as long as the increasing of time-lag.

The autocorrelation indicates the data are distributed randomly and stationary (Figure 9) and (Figure10). The amplitude of autocorrelation also does not show the critical value in upper and lower of zero value as the data boundary (reflected by the blue line). This could be as the indicator of low-correlated between the data.

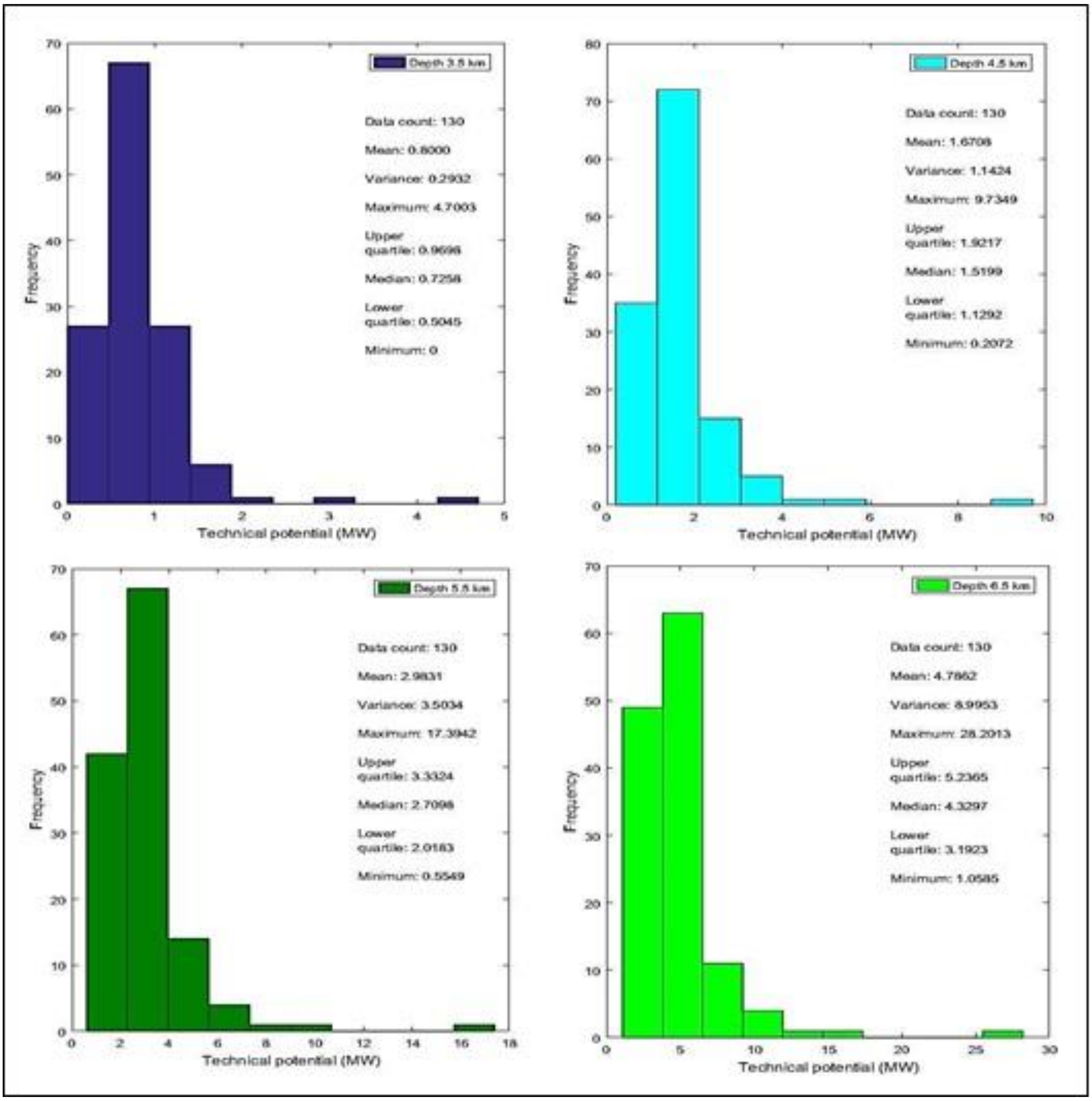


**Figure 8**. The Histogram Bar Charts of 3.5 km to 6.5 km depth slice

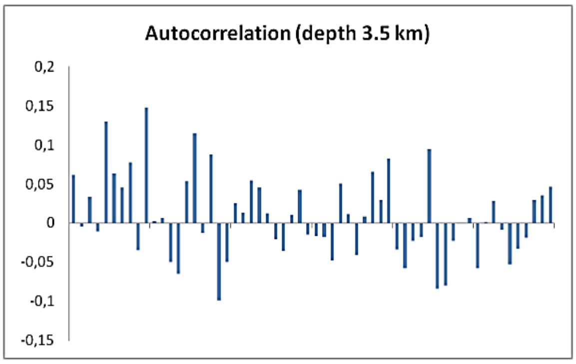


**Figure 9.** Autocorrelation result test at depth 3.5 km

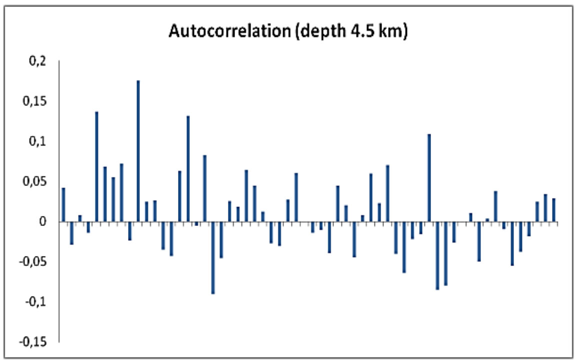


**Figure 10.** Autocorrelation result test at depth 4.5 km

### Spatial Relationship

The spatial relationships were described by covariance and variogram to assist in choosing lag-numbers and lag-separation of kriging estimation. The ordinary kriging is chosen due to the condition of stationary of the data based on previous autocorrelation analysis. The kriging is aimed to estimate values of the technical potential of an unsampled location with minimized variance.

### Theoretical Variogram Analysis

The theoretical variogram analysis was conducted in 3.5 km and 4.5 km depth due to the recommendation depth for drilling (Figure 11) and (Figure 12). The data visualize the covariance and semivariogram to know the prediction error value. The covariance is a statistical measure of the linear association between two random variables X and Y (Lee, C.F. et al., 2000). Whereas, semivariogram is a function that relates semivariance to sampling lag (Curran, P.J., 1988). This function can be estimated using remotely sensed data or ground data and represented as a plot that gives a picture of the spatial dependence of each point on its neighbor. As the result analysis, the prediction error in 3.5 km depth is 0.000719 and 0.000828 in 4.5 km depth, respectively.

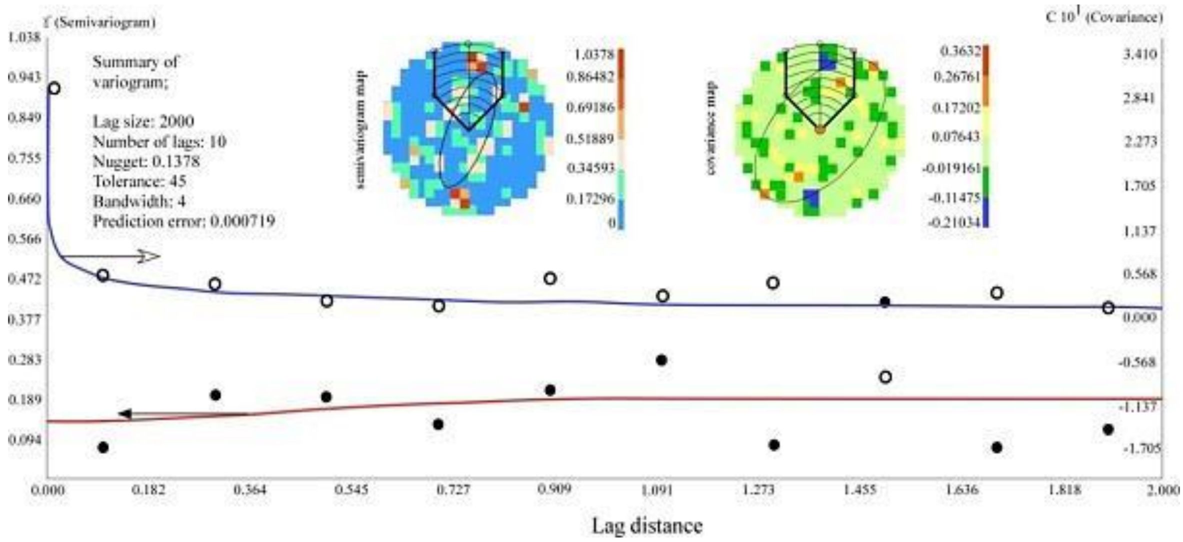


**Figure 11**. The Theoretical Variogram in 3.5 km depth

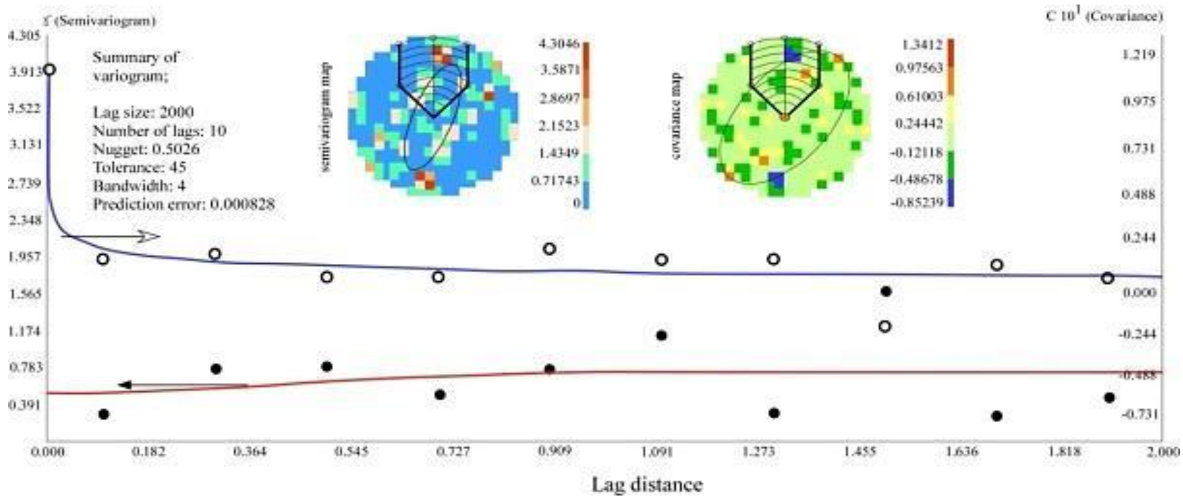


**Figure 12**. The Theoretical Variogram in 4.5 km depth

**CONCLUSION**

The Central Sumatra Basin has the potential for Enhanced Geothermal Systems (EGS) Utilization. The technical potential was classified into two slice depths that are 3.5 and 4.5 km. This was consider due to the thickness of sedimentary rock was 2,542 m and the basement rock could produce higher heat generation than sedimentary rock.

The recommended depth to drill is started from 2,600 m, which is 3.5 km and 4.5 km depth, have the low error correction and variance deviation.

The Technical Potential in Central Sumatra Basin was calculated by using the Beardsmore Protocol. The calculation was used the average cycle thermal efficiencies for a range of inlet fluid temperatures from 150 to 350°C. In 3.5 km depth, the lowest Technical Potential in this depth is 0.5 MW and the highest is 4.7 MW. In 4.5 km depth, the lowest Technical Potential is 0.66 MW and the highest is 5.76 MW. The total of technical potential in 3.5 km and 4.5 km depths are 103.5 MW and 217.9 MW, respectively. This potential could be used to fulfill the energy demands in Central Sumatra Area.

**REFERENCE**


Beardsmore, G.R., Rybach, L., Blackwell, D. and Baron, C., 2010. A protocol for estimating and mapping global EGS potential. GRC Transactions. 34. p. 301-312.

Busby, J. and Terrington, R., 2017. Assessment of the resource base for engineered geothermal systems in Great Britain. Geothermal Energy. 5(1). p. 7.

Clauser, C., 2006. Geothermal energy. Landolt-Börnstein, group VIII: advanced materials and technologies, 3, p. 493-604.

Curran, P. J., 1988. The Semivariogram in Remote Sensing: An Introduction. Remote Sensing of Environment. 24(3). p. 493-507.

Eubank, R.T. and Makki, A.C., 1981. Structural Geology of the Central Sumatra Back-arc Basin. Indonesian Petroleum Association, Proceeding 10th Annual Convention, p. 153-196.

Heidrick, T.L. and Aulia, K., 1993. A structural and Tectonic Model of The Coastal Plain Block, Central Sumatera Basin, Indonesia. Indonesian Petroleum Association, Proceeding 22th Annual Convention, 1, p. 285-316.

Hendrawan, R.N. and Draniswari, W.A., 2016. Assessing the possibility of Enhanced Geothermal System in western Indonesia. IOP Conference Series: Earth and Environmental Science. Sci. 42. 012021.

Lee, C. F., Lee, J. C., and Lee, A. C., 2000. Statistics for business and financial economics. World Scientific. 1. Singapore. p. 712.

Limberger, J., Calcagno, P., Manzella, A., Trumpy, E., Boxem, T., Pluymaekers, M.P.D. and van Wees, J.D., 2014. Assessing the prospective resource base for enhanced geothermal systems in Europe. Geothermal Energy Science. 2(1). p. 55.

Pambudi, N.A., 2017. Geothermal power generation in Indonesia, a country within the ring of fire: Current status, future development and policy. Renewable and Sustainable Energy Reviews. 81, p. 2893-2901.

Royal Holloway South East Asia Research Group. All Heat Flow Data (Open Access). (http://searg.rhul.ac.uk/current-research/heat-flow/, accessed November, 20th 2017)

Rybach, L., 2010. The future of geothermal energy and its challenges. Proceedings World Geothermal Congress Bali 2010, 29, p. 4.

Slagstad, T., 2008. Radiogenic heat production of Archaean to Permian geological provinces in Norway. Norwegian Journal of Geology, 88, p. 149-166.

Tester, J. W., Anderson, B. J., Batchelor, A. S., Blackwell, D. D., DiPippo, R., Drake, E. and Petty, S., 2006. The future of geothermal energy: Impact of enhanced geothermal systems (EGS) on the United States in the 21st century. *Massachusetts Institute of Technology*, p. 209.

Van Wees, J., Boxe, T., Angeloni, L., and Duas, P., 2013. A Prospective Study on the Geothermal Potential in the EU. *Geoelect Report*.

Submitted : May 23, 2019
Reviewed : June 18, 2019
Accepted : August 28, 2019